ChemComm

COMMUNICATION

View Article Online
View Journal | View Issue

Cite this: *Chem. Commun.*, 2025, **61**, 13413

Received 9th May 2025,
Accepted 22nd July 2025

DOI: 10.1039/d5cc02645h

rsc.li/chemcomm

A clickable spherical nucleic acid probe for fluorescence and synchrotron radiation X-ray dual-modality imaging†

Xiaobo Wang,[af] Xin Yan,[af] Feng Zhou,[af] Qiaowei Tang,[d] Zijian Xu,[b] Jichao Zhang,[b] Yong Guan,[e] Yanhong Sun,[c] Ying Zhu,[c] Jun Hu[abc] and Xiaoqing Cai*[abf]

In this study, we have developed a dual-mode probe based on click chemistry for spherical nucleic acids (SNAs), achieving extremely specific fluorescence imaging and synchrotron X-ray microscopy of neuronal cells.

The primary challenge in current bioimaging technologies is the difficulty in achieving molecular specificity alongside high spatial resolution using a single imaging modality.[1] While fluorescence microscopy achieves single-molecule detection sensitivity through targeted molecular labeling, it is limited by its poor tissue penetration (<200 μm) and vulnerability to photobleaching.[2,3] In contrast, synchrotron radiation scanning transmission X-ray microscopy (SR-STXM) exhibits high penetration, nanoscale spatial resolution and element specificity, enabling the analysis of the ultrastructure of tissues and cells and providing the sensitivity and spatial resolution required at the subcellular level.[4] However, it lacks specific molecular labeling methods. Combining the two techniques to design multimodal probes, particularly surface functionalized heavy metal nanomaterials, could become a crucial direction in addressing this bottleneck.

The high atomic number properties of gold nanoparticles create considerable contrast in synchrotron X-ray microscopy imaging.[5] These nanoparticles, functionalized for various applications, have found widespread use in areas such as biosensors, bioimaging, medical diagnosis, drug delivery, and clinical treatment, attributed to their exceptional biocompatibility, tunable stability, and low toxicity.[6,7] Spherical nucleic acids (SNAs) are spherical structures that modify nucleic acid molecules on the surface of nanoparticle cores. This structure imbues spherical nucleic acid probes with distinctive properties such as high stability, programmability, and multifunctionality. By meticulously designing nucleic acid sequences, SNAs can accurately label specific organelles or biomarkers through the use of targeted molecules such as aptamers or antibodies.[8] To date, a plethora of studies have been conducted on the self-stability,[9] contraction properties,[10] intracellular uptake,[11] extracellular uptake and intracellular distribution capability,[12] and tumor-targeted delivery function[13] of SNAs (Au SNAs) with gold nanoparticles (AuNPs) as their core. However, these studies primarily concentrate on the properties and functions of nucleic acid shells and have not explored their application in high contrast synchrotron X-ray imaging facilitated by the properties of the gold core.

Click chemistry is a category of highly efficient and specific chemical reactions, which mainly includes copper-catalyzed azide–alkyne cycloaddition (CuAAC), strain-promoted azide–alkyne cycloaddition (SPAAC), photo-induced thiol–ene reactions, and inverse electron-demand Diels–Alder (IEDDA) reactions.[14,15] These reactions are characterized by mild reaction conditions, high yields, and high selectivity, and have been widely applied in the fields of bioconjugation and molecular labelling.[16] By skillfully integrating click reactions with metabolic engineering, imaging probes can achieve highly specific and sensitive molecular labeling of cells.[17] Additionally, modifying alkynylated DNA on the surface of SNAs can facilitate specific covalent binding between probes and biological targets through click reactions. This approach not only significantly reduces nonspecific adsorption but also enables spatial and temporal control in complex biological systems.

Inspired by the concept of click chemistry, we have developed a novel type of click-on spherical nucleic acid probe

[a] *Shanghai Institute of Applied Physics, Chinese Academy of Sciences, Key Laboratory of Micro Interface Physics and Detection, Chinese Academy of Sciences, Shanghai 201800, China. E-mail: wangxiaobo@sinap.ac.cn, yanxin@sinap.ac.cn, zhoufeng@sinap.ac.cn*
[b] *Shanghai Synchrotron Radiation Facility (SSRF), Shanghai Advanced Research Institute, Chinese Academy of Sciences, Shanghai 201204, China. E-mail: xuzj@sari.ac.cn, zhangjc@sari.ac.cn, caixq@sari.ac.cn*
[c] *Institute of Materials Biology, Department of Chemistry, School of Science, Shanghai University, Shanghai 200444, China. E-mail: sunyanhong@shu.edu.cn, zhuying331@shu.edu.cn, hujun64@shu.edu.cn*
[d] *Xiangfu Laboratory, Jiaxing 314102, China. E-mail: tangqw_sinap@163.com*
[e] *University of Science and Technology of China, National Synchrotron Radiation Laboratory, Hefei 230029, China. E-mail: yongg@ustc.edu.cn*
[f] *University of Chinese Academy of Sciences, Beijing 100049, China*

† Electronic supplementary information (ESI) available. See DOI: https://doi.org/10.1039/d5cc02645h

(click-on SNA probe) with gold nanoparticles at its core. The DNA sequence is modified with alkynyl, fluorescent, and thiol groups to ensure the targeting ability and fluorescence imaging signal of the probe. This design aids in effectively controlling the particle size, preventing probe aggregation and fluorescence signal quenching, and providing strong signals for X-ray imaging. This allows us to achieve dual-mode imaging of fluorescence and STXM on PC12 cells and primary neuronal cells, respectively. In this study, we developed a new click-on SNA dual-mode imaging probe and used it to label neuronal cells for fluorescence and synchrotron radiation imaging, thereby verifying the practicality of the probes.

We initially designed a DNA sequence (alkyne-TTTTTTTT-iCy5-TTTTTTTT-SH) modified with click reaction functional groups (alkyne), a fluorescent group (Cy5), and a thiol group (SH). We then synthesized click-SNA probes using the salt aging method.[18] The concentration of NaCl in the solution plays a crucial role in the composition of click-SNA probes (Fig. 1A). Once the probes were successfully prepared, we connected it through a click reaction for cell labeling and imaging (Fig. 1B). Azidohomoalanine (AHA) is a non-classical amino acid analogue of methionine, distinguished by its propensity to randomly incorporate azide groups into methionine sites within synthetic proteins during the process of translation.[19] Given that transmembrane proteins are typically abundant in methionine,[20] this leads to an increased enrichment of AHA in membrane protein synthesis and transport pathways. Tetraacetylated *N*-azidoacetylmannosamide (Ac4ManNAz) is a metabolic glycoprotein labeling reagent containing an azide. It can be incorporated into the cellular sialic acid biosynthesis pathway, promoting the expression of azide sialic acid in cells.[21] Fig. 1C shows a schematic diagram depicting the probe labeling on the cell membrane *via* a click reaction. This process entails modifying the cell membrane with Ac4ManNAz azides through a biosynthetic pathway.

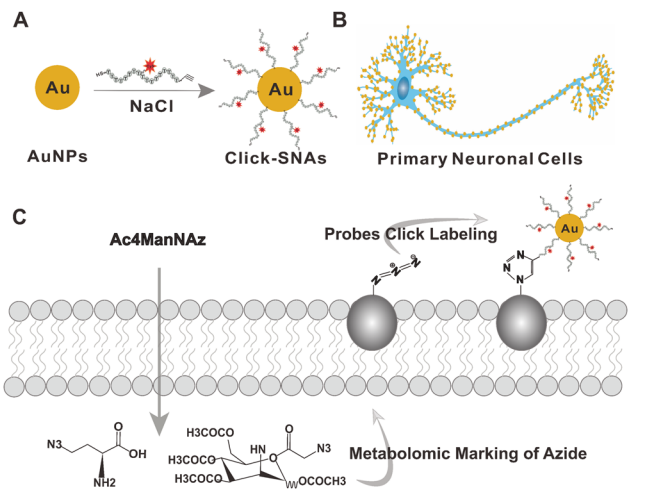

Fig. 1 Schematic diagram of the preparation and labeling of probes. (A) Preparation of click-SNA probes; (B) probe labeling on a primary neuronal model; (C) click reaction to implement the probe labeling process on the cell membrane.

We selected 5 nm AuNPs as the core for spherical nucleic acid probes and then utilized TEM and dynamic light scattering (DLS) to characterize the structure and size of the click-SNA probes. Furthermore, we measured their fluorescence emission spectra. From the TEM imaging results, it is clear that the click-SNA probes (Fig. 2B) exhibit a distinct nucleic acid molecule coupling structure on their periphery, in contrast to AuNPs (Fig. 2A). The particle sizes of the probes in the TEM images were statistically analyzed, showing particle sizes of approximately 5.57 nm for AuNPs and particle sizes of approximately 6.25 nm for click-SNA probes (Fig. 2C). Furthermore, the hydrodynamic diameter of the click-SNA probes was observed to be around 10 nm, which is larger than the hydration particle size of AuNPs (approximately 7 nm) (Fig. 2D). The emission spectrum of the click-SNA probes was also measured, demonstrating sufficient fluorescence intensity at 667 nm (Fig. 2E). These findings suggest that the synthesized click-SNA probes exhibit uniform particle size, no aggregation, and a fluorescence signal, indicating successful synthesis of the probe.

Following successful preparation of the probes, we initially carried out fluorescence and probe labeling on PC12 cells and primary neuronal cells for fluorescence imaging (Fig. 3). We co-cultured PC12 cells with 1 mM AHA for 12 hours and primary neuronal cells with 500 μM Ac4ManNAz for the same duration to induce azide incorporation into cellular metabolic expression.[22] For the purpose of conducting neuronal cell imaging, we extracted primary neurons from fetal mice using 18-day pregnant SD rats. We isolated separate cortical tissue blocks from fetal mice and prepared neuronal cultures using resuspension enzymatic hydrolysis. The neuronal cells were seeded at a density of 15 000–45 000 cells cm^{-2} in a poly(L-lysine)

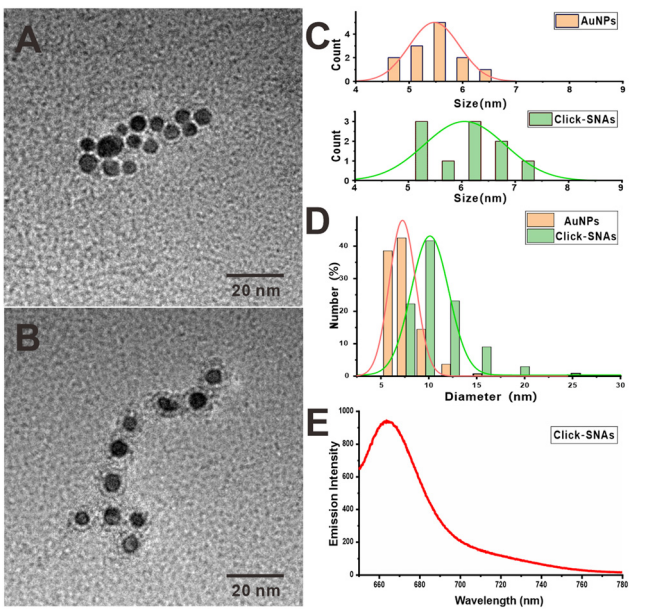

Fig. 2 Characterization of click-SNA probes. (A) Transmission electron microscopy (TEM) imaging of gold nanoparticles (AuNPs); (B) TEM imaging of click-SNA probes; (C) particle size statistics from TEM images; (D) particle size statistics from dynamic light scattering (DLS) measurements of click-SNA probes; (E) emission spectra of click-SNA probes.

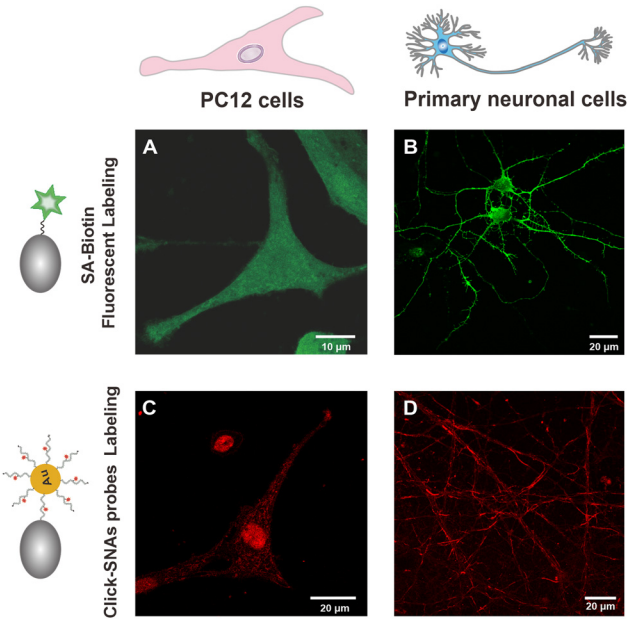

Fig. 3 Fluorescence imaging of PC12 cells (AHA) and neuronal cells (Ac4ManNAz). (A) Alkyne biotin, SA-AF488 click immunohistochemistry-labeled PC12 cell fluorescence imaging; (B) alkyne biotin, SA-AF488 click immunohistochemistry-labeled primary neuronal cell fluorescence imaging; (C) click-SNA probe-labeled fluorescence imaging of PC12 cells; (D) click-SNA probe-labeled fluorescence imaging of primary neuronal cells.

coated conical dish, and the neurobasal medium (supplemented with the B27 system) was replaced every 3 days. After 14 days of cell maturation, we conducted azide modification and fluorescence imaging labeling.[23]

After incorporating azide into the cell, we first utilized the strain-promoted azide–alkyne cycloaddition (SPAAC) reaction to couple biotin. Subsequently, we employed the biotin–streptavidin reaction to fluorescently label the cell using the Alexa Fluor™ 488 streptavidin conjugate (SA-AF488) (Fig. 3A and B). This enabled us to clearly distinguish the basic morphology of PC12 cells and the fine fibrous specialized structures of primary neurons. The results demonstrated that AHA and Ac4ManNAz were completely expressed in the cells. The application of AHA and Ac4ManNAz for the azide modification of cells can be effectively utilized to observe cell morphology.

Subsequently, we utilized click-SNA probes to label and image cells *via* click reactions (Fig. 3C and D). The imaging results enabled the observation of the basic morphological structure of both cell types. However, compared to the fluorescence imaging achieved through biotin–streptavidin coupling, the fluorescence signal intensity after probe labeling was inconsistent. This discrepancy may be attributed to the larger size and lower concentration of the probes, resulting in fewer probes being coupled to the cells, leading to a suboptimal imaging effect. From the fluorescence imaging results of PC12 cell probe labeling, it is evident that the nucleus exhibits a robust fluorescence signal. We hypothesize that this phenomenon is due to AHA's propensity to randomly integrate methionine sites into all newly synthesized proteins. This includes nuclear proteins such as histones, transcription factors, nuclear cytoskeleton, and nuclear porins, consequently generating strong fluorescence signals in the nucleus (Fig. 3C).[24] Conversely, Ac4ManNAz primarily engages in the synthesis of sialic acid on the neuronal cell membrane. No nuclear signal is observed following the labeling of cells with click-SNA probes (Fig. 3D).

Finally, we utilized click-SNA probes to label two types of cells for synchrotron radiation scanning transmission X-ray microscopy (SR-STXM) imaging (Fig. 4). We employed STXM to scan and probe the labeled cells with photons at 520 eV energy, observing the cell morphology through imaging contrast[25] (Fig. 4A). The STXM imaging results of PC12 cells showed that the nuclei labeled with AHA metabolism incubation also exhibited strong X-ray signals, and even the nucleolar structures could be clearly distinguished (Fig. 4B),[26] corroborating the fluorescence imaging results. Subsequently, we performed neuronal absorption edge imaging (Fig. 4C) and STXM imaging (Fig. 4D) in the National Synchrotron Radiation Laboratory (NSRL) BL07W soft X-ray Imaging Beamline Station and the Shanghai Light Source (SSRF) BL08U1A soft X-ray Spectroscopy Fiber Line Station, respectively, enabling us to visualize the neuronal cell fiber structure in detail.

In this study, the click-SNA probe-labeled cells exhibited a specific fluorescence signal, and well-defined specialized structures of neuronal fibers were observed using synchrotron X-ray microscopy. This indicates that the probes can effectively label PC12 cells and neuronal cells, thereby enabling dual-mode imaging through fluorescence and synchrotron radiation scanning transmission X-ray microscopy imaging.

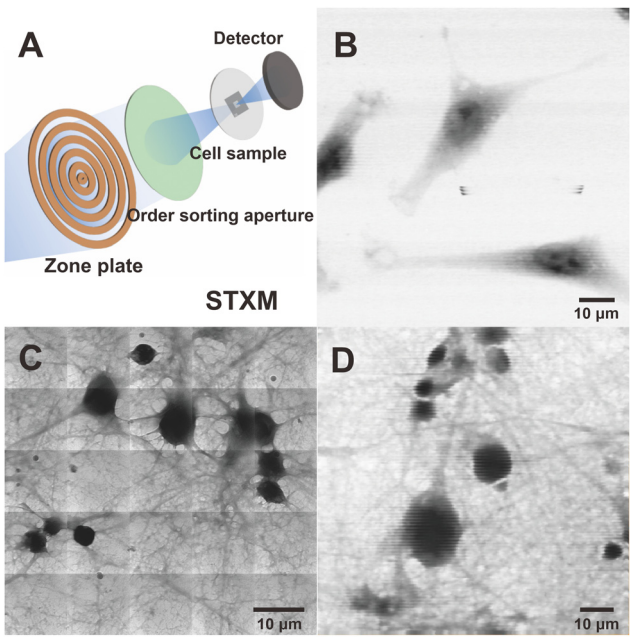

Fig. 4 Synchrotron radiation X-ray imaging of PC12 cells (AHA) and neuronal cells (Ac4ManNAz). (A) Schematic diagram of STXM imaging; (B) STXM imaging of PC12 cells labeled with click-SNA probes (SSRF); (C) absorption edge imaging of primary neurons labeled with click-SNA probes (NSRL); (D) STXM imaging of primary neurons labeled with click-SNA probes (SSRF).

In conclusion, this study innovatively developed a multimodal molecular probe, click-SNAs, which is based on the synergistic effect of click chemistry and spherical nucleic acids. It successfully achieved high specificity fluorescence and synchrotron X-ray dual-mode imaging of PC12 cells and primary neuronal cells. For the first time, this probe combines the gold core characteristics of spherical nucleic acids with the efficient coupling of click chemistry, significantly enhancing the labeling specificity of synchrotron X-ray imaging and facilitating fluorescence multimodal imaging. This research achievement not only provides new insights for the design of synchrotron X-ray imaging probes but also opens up new avenues for the study of brain neuron-specific labeling imaging. Looking forward, the labeling strategy based on click chemistry is anticipated to be more widely applied in the field of synchrotron radiation imaging. The modular design concept of click-SNA probes is likely to provide robust technical support for three-dimensional analysis research at the mesoscale of the whole brain.

CRediT: Xiaoqing Cai supervised this study. Xiaobo Wang carried out the experiments, organized the data, and drafted the manuscript. Xin Yan, Feng Zhou, and Qiaowei Tang provided guidance and assistance during the experimental operations. Zijian Xu, Jichao Zhang, and Yong Guan provided guidance on X-ray microscopy. Yanhong Sun and Ying Zhu conducted critical revisions. Jun Hu and Xiaoqing Cai analyzed the data and drafted the manuscript. All authors engaged in discussions and provided comments on the manuscript.

This research was supported by the National Key R&D Program of China (2021YFA1200904, 2022YFA1603702 and 2021YFA1601001), the National Natural Science Foundation of China (12335019 and 11875316) and the Chinese Academy of Sciences' study on open large-scale infrastructure. We also wish to extend our sincere gratitude to the Shanghai Synchrotron Radiation Facility (SSRF, China), particularly the BL08U1A Soft X-ray Spectromicroscopy Beamline (**https://cstr.cn/31124.02.SSRF.BL08U1A**) and the Shanghai Light Source Experimental Assistance System (**https://cstr.cn/31124.02.SSRF.LAB**). Additionally, we appreciate the support from the National Synchrotron Radiation Laboratory (NSRL, China), particularly the BL07W Soft X-ray Imaging Beamline Station. Furthermore, we are immensely thankful to the National Protein Science Research (Shanghai) Facility (**https://cstr.cn/31129.02.NFPS**) and the Biological Small Angle X-ray Scattering Station (BL19U2, **https://cstr.cn/31129.02.NFPS.BL19U2**) for their technical support and assistance in data collection and other aspects of the research.

Conflicts of interest

There are no conflicts to declare.

Data availability

All experimental source data (Probe characterization and Imaging data) are stored on the Science Data Bank platform. Refer to DOI: **https://doi.org/10.57760/sciencedb.j00186.00704**.

References

1 J. H. Zhao, J. W. Chen, S. N. Ma, Q. Q. Liu, L. X. Huang, X. N. Chen, K. Y. Lou and W. Wang, *Acta Pharm. Sin. B*, 2018, **8**, 320–338.
2 Y. X. Ma, Q. H. Chen, X. Y. Pan and J. Zhang, *Top. Curr. Chem.*, 2021, **379**, 10.
3 Y. K. G. Kooh and N. Huebsch, *arXiv*, 2025, preprint, arXiv:2502.03661v1, DOI: **10.48550/arXiv.2502.03661**.
4 C. Y. Zhang, H. Eraky, S. Q. Tan, A. Hitchcock and D. Higgins, *ACS Nano*, 2023, **17**, 21337–21348.
5 R. D. Ross, L. E. Cole, J. M. R. Tilley and R. K. Roeder, *Chem. Mater.*, 2014, **26**, 1187–1194.
6 J. N. Fan, Y. Q. Cheng and M. T. Sun, *Chem. Rec.*, 2020, **20**, 1474–1504.
7 M. Yaseen, M. Humayun, A. Khan, M. Usman, H. Ullah, A. A. Tahir and H. Ullah, *Energies*, 2021, **14**, 1278.
8 J. R. Ferrer, J. A. Wertheim and C. A. Mirkin, *Bioconjugate Chem.*, 2019, **30**, 944–951.
9 M. E. Kyriazi and A. G. Kanaras, *Colloidal Nanopart. Biotechnol.*, 2018, **10507**, 105070A.
10 G. Q. Wang, L. Yu, Y. Akiyama, T. Takarada and M. Maeda, *Biotechnol. J.*, 2018, **13**, 12.
11 A. C. Wong and D. W. Wright, *Small*, 2016, **12**, 5592–5600.
12 B. Malile, J. Brkic, A. Bouzekri, D. J. Wilson, O. Ornatsky, C. Peng and J. I. L. Chen, *ACS Appl. Bio Mater.*, 2019, **2**, 4316–4323.
13 C. Xue, S. Y. Hu, Z. H. Gao, L. Wang, M. X. Luo, X. Yu, B. F. Li, Z. F. Shen and Z. S. Wu, *Nat. Commun.*, 2021, **12**, 2928.
14 L. Taiariol, C. Chaix, C. Farre and E. Moreau, *Chem. Rev.*, 2022, **122**, 340–384.
15 N. K. Devaraj and M. G. Finn, *Chem. Rev.*, 2021, **121**, 6697–6698.
16 Q. Tang, D. Yin, Y. Liu, J. Zhang, Y. Guan, H. Kong, Y. Wang, X. Zhang, J. Li, L. Wang, J. Hu, X. Cai and Y. Zhu, *JACS Au*, 2024, **4**, 893–902.
17 J. D. Zheng, Q. Q. Zhan, L. J. Jiang, D. Xing, T. Zhang and K. L. Wong, *Inorg. Chem. Front.*, 2020, **7**, 4062–4069.
18 H. Pei, F. Li, Y. Wan, M. Wei, H. J. Liu, Y. Su, N. Chen, Q. Huang and C. H. Fan, *J. Am. Chem. Soc.*, 2012, **134**, 11876–11879.
19 R. Hatzenpichler, S. Scheller, P. L. Tavormina, B. M. Babin, D. A. Tirrell and V. J. Orphan, *Environ. Microbiol.*, 2014, **16**, 2568–2590.
20 C. Y. Li, S. Takazaki, X. R. Jin, D. C. Kang, Y. Abe and N. Hamasaki, *Biochemistry*, 2006, **45**, 12117–12124.
21 S. S. Han, D. E. Lee, H. E. Shim, S. Lee, T. Jung, J. H. Oh, H. A. Lee, S. H. Moon, J. Jeon, S. Yoon, K. Kim and S. W. Kang, *Theranostics*, 2017, **7**, 1164–1176.
22 D. E. Sun, X. Q. Fan, Y. J. Shi, H. Zhang, Z. M. Huang, B. Cheng, Q. Tang, W. Li, Y. T. Zhu, J. Y. Bai, W. Liu, Y. Li, X. T. Wang, X. G. Lei and X. Chen, *Nat. Methods*, 2021, **18**, 107–113.
23 G. Aakalu, W. B. Smith, N. Nguyen, C. G. Jiang and E. M. Schuman, *Neuron*, 2001, **30**, 489–502.
24 C. Turberville and V. M. Craddock, *Biochem. J.*, 1971, **124**, 725–739.
25 C. P. Wang, Z. J. Xu, H. G. Liu, X. Tao and R. Z. Tai, *Nucl. Sci. Tech.*, 2017, **28**, 6.
26 W. Meyer-Ilse, D. Hamamoto, A. Nair, S. A. Lelièvre, G. Denbeaux, L. Johnson, A. L. Pearson, D. Yager, M. A. Legros and C. A. Larabell, *J. Microsc.*, 2001, **201**, 395–403.

